SLAC-PUB-6522
June 1994
(A/E)

Emittance Dilution by Ions in the SLC Arcs*

P. Emma, T. Raubenheimer, F. Zimmermann
Stanford Linear Accelerator Center, Stanford University, Stanford, CA 94309, USA

Abstract
Since the start of flat-beam operation in 1993 typical vertical IP spot sizes in the SLC are well below 1 micron, and the luminosity is highly sensitive to dilutions of the vertical emittance. In the arcs, the ionization of the residual gas by the bunch head gives rise to an ion cloud, whose electric field deflects the tail of the bunch and may cause an unrecoverable filamentation in phase space. The effect of the ions is particularly important in regions with large dispersion, due to the strong correlation of energy and longitudinal position within a bunch. Computer simulations of a bunch passage in the presence of ions have been performed to estimate the magnitude of the emittance dilution.

1 INTRODUCTION

In 1994, the SLC will be operating with flat beams [1] and with a new final focus [2]. In the flat beam mode, the normalized vertical emittance is reduced from the original design of 30 mm-mrad to 3 mm-mrad and, with the new final focus, the vertical beam size at the interaction point should be reduced from 1.5 μm to roughly 500 nm.

To reach the IP, the beams are accelerated in the SLAC linac to 50 GeV and then transported 1.2 km through the SLC arcs. The original vacuum pressure tolerance in the arcs was 1×10^{-7} torr; this was estimated from considerations of the increased focusing at the beam tail due to ions created by the head of the beam [3, 4]. Because of the smaller vertical emittances, a reevaluation of the acceptable vacuum pressure has become necessary. Simply scaling the tolerance with the decreased beam emittance would suggest a vacuum tolerance of 3×10^{-5} torr; the focusing scales inversely with the square root of the emittance. In this paper, we describe another source of emittance dilution that sets a comparable vacuum tolerance.

When the beam is accelerated in the SLAC linac, transverse wakefields deflect the tail of a bunch, and longitudinal wakefields and the accelerating rf cause the bunch energy to be correlated with the longitudinal position z in the bunch. Either the transverse wakefields or the correlated energy deviation, along with vertical dispersion, will lead to y-z correlations. With such a correlation, the tail of the beam will encounter a dipole deflecting field due to the ions created by the head of the bunch; this is illustrated schematically in Fig. 1.

2 SLC ARCS

The SLC arcs transport the beam from the end of the linac to the final focus. They are constructed from 22 achromats, each achromat consisting of 10 FODO cells using combined function bending magnets. The length of the SLC arcs is $L \approx 1200$ m, the average beam sizes are $\sigma_x \approx 50$ μm, $\sigma_y \approx 15$ μm, and $\sigma_z \approx 0.8$ mm, and the average beta functions $\beta_{x,y} \approx 4$ m. The average value of the horizontal dispersion is 40 mm, and, since the arcs are not planar, some vertical dispersion exists by design. In addition, because of difficulties in matching, there is typically a 10 mm dispersion mismatch at the entrance of the arcs that oscillates as a free betatron oscillation to the end. The vacuum pressure profile is not constant throughout the arc, but exhibits variations of two orders of magnitude with sharp dips at the pump locations (see Fig. 2). The actual pressure pattern contains frequency components in resonance with harmonics of the betatron frequency, and thus can cause a larger emittance increase than expected for constant pressure.

Finally, the beam from the SLAC linac has both a correlated energy deviation due to the rf curvature and the longitudinal wakefields and an uncorrelated energy spread. The typical correlated energy deviation is $\Delta E/E \approx 2 \times 10^{-3}$, while the uncorrelated relative energy spread is roughly $\delta_{inc} \approx 5 \times 10^{-4}$.

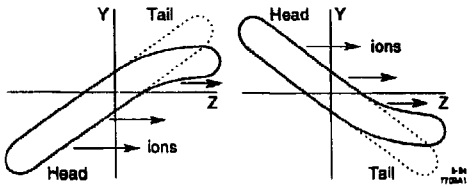

Figure 1: Schematic picture of resonant tail excitation for two different betatron phases.

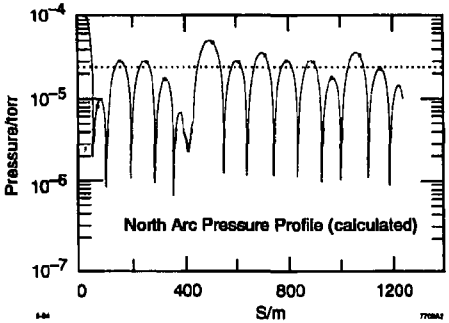

Figure 2: Pressure profile in the SLC north arc calculated according to [5]. The dips are the pump locations. The circles indicate newly installed vacuum gauges.

*Work supported by Department of Energy contract DE-AC03-76SF00515.

Presented at the Fourth European Particle Accelerator Conference (EPAC'94), London, England, June 27-July 1, 1994

3 IONS

3.1 Generation

In the SLC arcs, the ions are generated by collisional ionization. At 50 GeV, the cross section for ionization of CO is roughly $\sigma_{ion} \approx 2\,\mathrm{Mb}$. With a bunch charge of 3.5×10^{10} and a vacuum pressure of 1×10^{-4} torr, the linear ion density is roughly $\lambda_{ion} = 2 \times 10^7$ ions/meter at the beam tail. Thus, with the typical beam sizes, the beam tail has an additional phase advance of $\Delta\Psi \approx 0.8$ and $\Delta\Psi_y \approx 3.0$.

To a good approximation, the produced ions do not change their position during the bunch passage. The ions move vertically by less than $\sigma_y/20$ during a time interval σ_z/c. Their distribution is thus directly given by the projected bunch distribution. On the contrary, the effect of the generated electrons on an electron bunch can be neglected, since they traverse up to 50 vertical sigma during the same period. The situation is different for the positron beam in the south arc where the atomic electrons are trapped inside the bunch. This introduces further complications that are not addressed in this paper.

3.2 Resonant Excitation of Beam

Because of the y-z correlation, the ion cloud produced by the head is displaced with respect to the bunch tail so that the electric field due to the ions deflects the tail. Assuming the correlation, and thus the excitation, oscillates at the betatron frequency, the effect on the bunch tail is accumulated as illustrated in Fig. 1.

We estimate this effect using a simple analytic model. The linearized equation of motion for the centroid of a slice at longitudinal position z is

$$y''(z) + K_1 y(z) = \int_{-\infty}^{z} K_{ion}(z,z')[y(z') - y(z)]dz', \quad (1)$$

where K_1 is the external focusing, and $K_{ion}\Delta y$ is the linear deflection due to the ions. In the absence of horizontal x-z correlations the function K_{ion} is

$$K_{ion} = N\lambda_{beam}(z')\frac{\sigma_{ion}\rho_{gas}r_e}{\gamma\sigma_y(\sigma_x+\sigma_y)}, \quad (2)$$

where $N\lambda_{beam}$ is the longitudinal beam particle distribution, ρ_{gas} is the vacuum gas density, and r_e is the classical electron radius.

We expand $y(z)$ in a perturbation series. Assuming a linear y-z correlation and smooth focusing, $y_0(z) = \hat{y}z/\sigma_z \cos(s/\beta + \phi)$, the first order effect of ions is

$$\hat{y_1}(z) = \frac{\hat{y}\beta L\lambda_{ion}r_e}{2\gamma\sigma_y(\sigma_x+\sigma_y)}\left[e^{-z^2/2\sigma_z^2} + \frac{z}{2\sigma_z}\left(1+\mathrm{erf}(\frac{z}{\sqrt{2}\sigma_z})\right)\right] \quad (3)$$

causing an emittance dilution of

$$\Delta\epsilon \approx \frac{1}{2\pi\beta}\left(\hat{y}\frac{L\beta\lambda_{ion}r_e}{2\gamma\sigma_y(\sigma_x+\sigma_y)}\right)^2. \quad (4)$$

The actual arcs are not this simple because there is a large x-z correlation due to horizontal dispersion and correlated energy spread. This turns out to be fortunate in that it significantly reduces the effects of the ions. We estimate this effect by including the next term in the expansion for the deflection which is proportional to $K_{ion}\Delta x^2\Delta y/\sigma_x^2$. This nonlinear term reduces the emittance dilution by $(2\hat{x}/\sigma_x)^2$ for $\hat{x} \gg \sigma_x$, where the x-z correlation is $\hat{x}z/\sigma_z$. In the SLC arcs, the ratio $\hat{x}/\sigma_x$ is ~ 1.6, and thus the emittance dilution is reduced by ~ 10.

3.3 Simulation Study

A more precise estimate of the emittance increase is obtained by a computer simulation, which takes into account the nonlinearity of the ion kick, optical functions, beam distribution in phase space, and the actual pressure profile along the arc. The simulation is performed as follows. The correlation between longitudinal position and energy (at that position) is assumed to be sinusoidal, $\delta(z) = \sqrt{2}\,\delta_{rms}\,\sin\left(\frac{\pi z}{2\sigma_z}\right)$, which is a good approximation to reality. The longitudinal and the transverse distributions are considered to be Gaussian. The bunch is decomposed longitudinally into 25–60 slices. At every position s_k a kick is applied to each slice, which is due to the ions generated by all the previous slices. The kick represents the integrated effect over the distance $s_k - s_{k-1}$. The kick on the j-th slice at position s_k is given by

$$\Delta y_j'(s_k) = -\sum_{i<j}\frac{\lambda_i r_e(s_k - s_{k-1})}{\gamma}\cdot \mathrm{Re}[F(x_i,x_j,y_i,y_j,s_k)]. \quad (5)$$

The change in x_j' is given by the imaginary part of the same formula. In Eq. (5) $x_i, x_j, y_i \ldots$ are the centroid coordinates of the slices, and λ_i denotes the number of ions generated by the i-th slice per m, given by $\lambda_i = \sigma_{ion}N_i\rho_{gas}$, where N_i is the number of electrons in slice i. The function F represents the kick from a Gaussian flat beam à la Bassetti-Erskine [7],

$$F(x_i,x_j,y_i,y_j,s_k) \equiv \left(\frac{2\pi}{\Sigma_{k,x}^2 - \Sigma_{k,y}^2}\right)^{\frac{1}{2}} \cdot \quad (6)$$

$$\cdot\left[W\left(\frac{x_j - x_i + i(y_j - y_i)}{(2\Sigma_{k,x}^2 - 2\Sigma_{k,y}^2)^{\frac{1}{2}}}\right) - \exp\left(-\frac{(x_j-x_i)^2}{2\Sigma_{k,x}^2} - \right.\right.$$
$$\left.\left. -\frac{(y_j-y_i)^2}{2\Sigma_{k,y}^2}\right)\cdot W\left(\frac{(x_j-x_i)\frac{\Sigma_{k,y}}{\Sigma_{k,x}} + i(y_j-y_i)\frac{\Sigma_{k,x}}{\Sigma_{k,y}}}{(2\Sigma_{k,x}^2 - 2\Sigma_{k,y}^2)^{\frac{1}{2}}}\right)\right],$$

where $\Sigma_{k,x,y}^2 \equiv 2\beta_{x,y}(s_k)\epsilon_{x,y} + 2\eta_{x,y}^2(s_k)\delta_{inc}^2$ is the sum of the squares of the sizes for slices i and j at the position s_k and $W(z) \equiv e^{-z^2}(1 - \mathrm{erf}(-iz))$ denotes the complex error function. Only the centroid coordinates of each slice are changed, not the size. The most important contribution to a change in size arises from the dependence of the vertical kick on the horizontal position.[6] This effect is small compared with the centroid change.

The sliced bunch is transported through a model of the arc, and the effective emittance increase is deduced from the shift of the individual slices with respect to

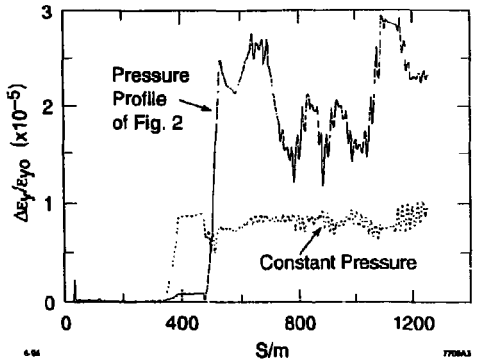

Figure 3: Relative increase of vertical emittance as a function of position along the arc for an average pressure of 2.2×10^{-5} torr. The two curves correspond to different pressure profiles.

each other, after subtracting the dispersive component of the transverse coordinates. It is convenient to introduce a 4×4 matrix σ by $\sigma_{j,k} \equiv < (x_j - < x_j >)(x_k - < x_k >) >$, where the $x_{j,k}$ are the centroid positions of the slices transformed to the beginning of the arc through the linear optics, and the square brackets denote an average over the bunch. The indices j and k represent the four transverse phase space dimensions. The design beam distribution is also characterized by a 4×4 matrix σ_0 related to the design emittances $\epsilon_{0,x,y}$ by $\epsilon^2_{0,x,y} = \det(\sigma_{0,x,y})$, where $\sigma_{0,x}$ and $\sigma_{0,y}$ are the 2×2 submatrices of σ_0 for the horizontal and vertical planes, respectively. The relative emittance increase caused by the ions is $\Delta\epsilon_{x,y}/\epsilon_{0,x,y} = \sqrt{\det(\sigma_{x,y} + \sigma_{0,x,y})}/\epsilon_{0,x,y}$. A typical emittance change during a bunch passage along the entire arc is presented in Fig. 3 both for a constant and for an actual pressure profile, with an average pressure of 2.2×10^{-5} torr each. In this particular example the real pressure profile leads to a three times larger emittance change. For different pressure values the opposite ratio has also been found.

3.4 *Tolerance for Pressure and Dispersion*

Figure 4 shows some results of the simulation which illustrate that the relative increase of the vertical emittance is approximately proportional to the square of the pressure and increases by more than two orders of magnitude if the amplitude of the dispersion mismatch changes from 0 to 25 mm. In Fig. 5 the pressure corresponding to a luminosity decrease of 1–10% is depicted as a function of the peak amplitude of the incoming dispersion. Since typically the latter is smaller than 15 mm, a pressure of 4×10^{-5} torr is sufficient to achieve a luminosity degradation of less than 1%. Note that part of the final y-z correlation can be corrected, which would loosen the pressure tolerance.

4 CONCLUSIONS

The resonant excitation by ionized atoms imposes a pressure tolerance of 4×10^{-5} torr in the SLC arcs. The peak

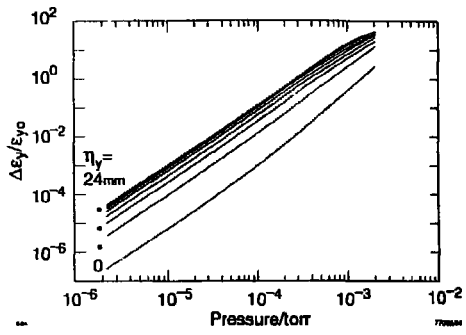

Figure 4: Relative increase of the vertical emittance along the entire arc as a function of the pressure, for different values of dispersion mismatch.

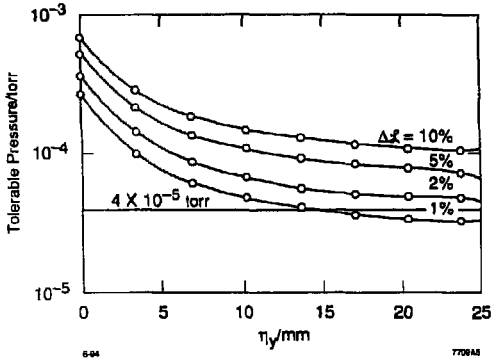

Figure 5: Pressure tolerance as a function of peak amplitude of mismatched vertical dispersion for different luminosity degradations.

amplitude of the mismatched vertical dispersion in the arcs should not exceed 15 mm. In April of 1994, twelve cold cathode vacuum gauges per arc were installed for adequate pressure monitoring.

5 ACKNOWLEDGEMENTS

We thank A. Chao, F.-J. Decker, M. Ross, W. Spence, and N. Walker for helpful discussions.

6 REFERENCES

[1] C. Adolphsen, *et al.*, *PAC 93*, Washington DC (1993).

[2] N. Walker, R. Helm, J. Irwin, and M. Woodley, *Proc. PAC 93*, Washington DC (1993).

[3] A. Chao, SLAC–CN–121 (1981).

[4] J. Rees, SLAC–CN–243 (1983).

[5] V. Ziemann, SLAC–PUB–5962 (1992).

[6] T.O. Raubenheimer and P. Chen, SLAC–PUB–5893 (1992).

[7] M. Bassetti and G. A. Erskine, CERN–ISR–TH/80–06 (1980).